

A New Paradigm for Precision Top Physics: Weighing the Top with Energy Correlators

Jack Holguin,¹ Ian Moult,² Aditya Pathak,³ and Massimiliano Procura⁴

¹*CPHT, CNRS, Ecole polytechnique, IP Paris, F-91128 Palaiseau, France*

²*Department of Physics, Yale University, New Haven, CT 06511*

³*University of Manchester, School of Physics and Astronomy, Manchester, M13 9PL, United Kingdom*

⁴*University of Vienna, Faculty of Physics, Boltzmannngasse 5, A-1090 Vienna, Austria*

Final states in collider experiments are characterized by correlation functions, $\langle \mathcal{E}(\vec{n}_1) \cdots \mathcal{E}(\vec{n}_k) \rangle$, of the energy flow operator $\mathcal{E}(\vec{n}_i)$. These correlation functions typically exhibit a power-law scaling characteristic of asymptotically free Quantum Chromodynamics. In this *Letter*, we show that the top quark imprints itself as a peak in the three-point correlation function at an angle $\zeta \sim m_t^2/p_T^2$, with m_t the top quark mass and p_T its transverse momentum. This provides direct access to one of the most important parameters of the Standard Model in one of the field theoretically simplest observables. We show that the three-point correlator allows us to simultaneously achieve high sensitivity to the top mass and high insensitivity to soft physics and underlying event contamination. We find it an amusing turn of fate that correlation functions which have received the most interest in the context of conformal field theories, in fact hold the key to understanding the heaviest known particle.

Introduction.—The Higgs and top quark masses play a central role both in determining the structure of the electroweak vacuum [1–3], and in the consistency of precision Standard Model fits [4, 5]. Indeed, the near-criticality of the electroweak vacuum may be one of the most important clues from the Large Hadron Collider (LHC) for the nature of beyond the Standard Model physics [2, 6–10]. This provides strong motivation for improving the precision of Higgs and top quark measurements.

While the measurement of the Higgs mass is conceptually straightforward both theoretically and experimentally [11], this could not be further from the case for the top mass (m_t). Due to its strongly interacting nature, a field theoretic definition of m_t , and its relation to experimental measurements, is subtle. In e^+e^- colliders, precision top mass measurements can be made from the threshold lineshape [12–19]. However, this approach is not possible at hadron colliders, where, despite the fact that direct extractions have measured m_t to a remarkable accuracy [20–23], there is a debate on the theoretical interpretation of the measured “Monte Carlo (MC) top mass parameter” [24]. This has been argued to induce an additional $\mathcal{O}(1 \text{ GeV})$ theory uncertainty on m_t . For recent discussions, see [25, 26]. It is therefore crucial to explore kinematic top-mass sensitive observables at the LHC where a direct comparison of the experimental data with first principles theory predictions can be carried out.

Significant progress has been made in this regard from multiple directions. First, in [27, 28] it was shown using soft-collinear effective theory (SCET) [29–32], and boosted heavy quark effective theory (bHQET) [33–38] that rigorous factorization theorems can be derived for event shapes measured on boosted top quarks, enabling these observables to be expressed in terms of the top quark mass in a field theoretically well defined mass scheme [39–43]. This approach can also be used to calibrate the MC top mass parameter [44–46]. Second, there

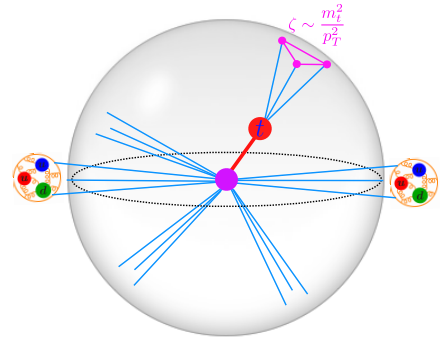


FIG. 1: A boosted top quark imprints its short lived existence onto the three-point correlator with a characteristic angle, $\zeta \sim (1 - \cos \theta)/2 \sim m_t^2/p_T^2$.

has been wide-ranging progress in parton shower algorithms capable of simulating fully exclusive events, both in terms of the general description of QCD showering [47–60], and the specific treatment of top production and decay [61–66].

A unique feature of the LHC is that large numbers of top quarks (as well as $W/Z/h$ bosons) are produced with sufficient boosts that they decay into single collimated jets on which jet shapes can be measured. Combined with the seminal introduction of robust jet algorithms [67–71], this initiated the field of jet substructure [72–74]. For reviews, see [75, 76]. In Ref. [77], the groomed [78, 79] jet mass was proposed as a top mass sensitive observable, enabling a realization of the factorization based approach of [27, 28]. For measurements, see [80, 81]. While jet grooming significantly improves the robustness of the observable, residual hadronization corrections [82] and contamination from the underlying event (UE) continue to be limiting factors in achieving a precision competitive with direct measurements.

In recent years, there has been a program to rethink [83] jet substructure directly in terms of correlation functions, $\langle \mathcal{E}(\vec{n}_1) \cdots \mathcal{E}(\vec{n}_k) \rangle$, of the energy flow in a direction \vec{n} [84–91], $\mathcal{E}(\vec{n})$, motivated by earlier work on the study of energy flow in conformal field theories (CFTs) [88–90, 92–94], which has also seen a revival in the context of the conformal bootstrap [91, 95–99].¹ These correlators have a number of remarkable properties as compared with standard jet shapes. Most importantly for phenomenological applications, correlators are insensitive to soft radiation even without the application of a grooming algorithm. They can also be computed on tracks [83, 110, 111], using the formalism of track functions [112, 113], which allows for higher angular resolution and suppresses pile-up. More theoretically, their structure enables the use of symmetries and the light-ray operator product expansion (OPE) [88, 91, 95–97]. However, so far their application to jet substructure has been restricted to massless quark or gluon jets [83, 114–117].²

In this *Letter*, we present a new paradigm for precision top mass measurements with jet substructure based on the simple idea of exploiting the mass dependence of the characteristic opening *angle* of the decay products of the boosted top, $\zeta \sim m_t^2/p_T^2$ (see Fig. 1), rather than directly measuring the jet mass. The motivation for rephrasing the question in this manner is twofold. First, this angle can be accessed via low point correlators, which are simpler field theoretically. Second, while the jet mass is sensitive to soft contamination and UE, the angle ζ is not, since it is primarily determined by the hard dynamics of the top decay. In the following, we will show that the three-point correlator in the vicinity of $\zeta \sim m_t^2/p_T^2$ provides a simple, but highly sensitive probe of the top quark mass, free of the typical challenges of jet-shape based approaches.

The Three-Point Energy Correlator.—There has recently been significant progress in understanding the perturbative structure of correlation functions of energy flow operators. This includes the calculation of the two-point correlator at next-to-leading order (NLO) in QCD [124, 125] and NNLO in $\mathcal{N} = 4$ super Yang-Mills [92, 126], as well as the first calculation of a three-point correlator [115], which was further analyzed in [52, 116, 117]. The idea of using the three-point correlator to study the top quark is a natural one, and was considered early on in the jet substructure literature [127]. However, only due to this recent theoretical progress have energy correlators been proposed as precision jet substructure observables [83, 128], opening the door to their use for Standard Model measurements.

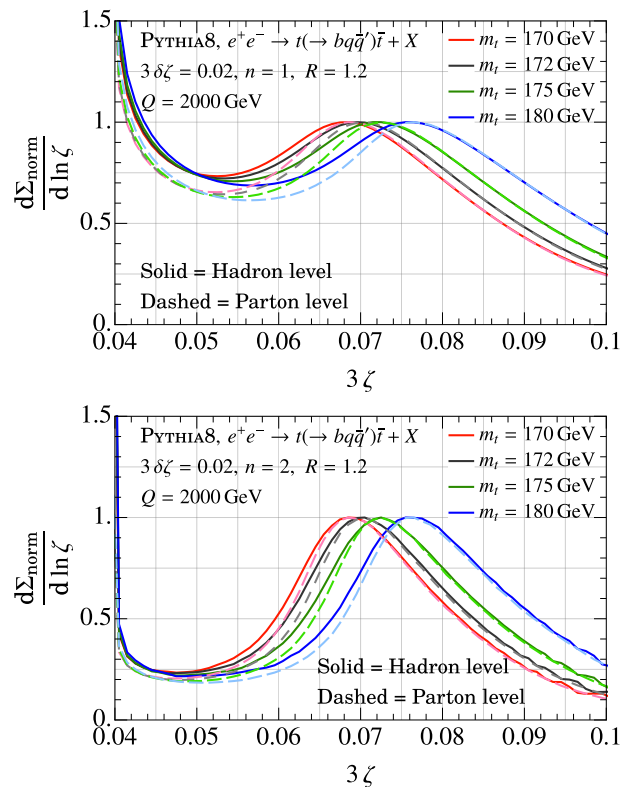


FIG. 2: The $n = 1, 2$ three-point correlators on boosted tops in e^+e^- showing a clear peak at $\zeta \sim 3m_t^2/Q^2$. All graphs are normalized to peak height.

The three-point correlator (EEEC) with generic energy weights is defined, following the notation in [115], as

$$G^{(n)}(\zeta_{12}, \zeta_{23}, \zeta_{31}) = \int d\sigma \widehat{\mathcal{M}}^{(n)}(\zeta_{12}, \zeta_{23}, \zeta_{31}), \quad (1)$$

with the measurement operator given by

$$\widehat{\mathcal{M}}^{(n)}(\zeta_{12}, \zeta_{23}, \zeta_{31}) = \sum_{i,j,k} \frac{E_i^n E_j^n E_k^n}{Q^{3n}} \delta(\zeta_{12} - \hat{\zeta}_{ij}) \delta(\zeta_{23} - \hat{\zeta}_{ik}) \delta(\zeta_{31} - \hat{\zeta}_{jk}). \quad (2)$$

Here $\hat{\zeta}_{ij} = (1 - \cos(\theta_{ij}))/2$, with θ_{ij} the angle between particles i and j , the sum runs over all triplets of particles in the jet, and Q denotes the hard scale in the measurement. The EEEC is not an event-by-event observable, but rather is defined as an ensemble average.

We are interested in the limit $\zeta_{12}, \zeta_{23}, \zeta_{31} \ll 1$, such that all directions of energy flow lie within a single jet. In the case of a CFT (or massless QCD up to the running coupling), the EEEC simplifies due to the rescaling symmetry along the light-like direction defining the jet. In this case, the EEEC can be written in terms of a scaling variable, ζ_{31} and two cross ratios $z\bar{z} = \zeta_{12}/\zeta_{31}$, $(1-z)(1-\bar{z}) = \zeta_{23}/\zeta_{31}$,

$$G^{(1)}(\zeta_{12}, \zeta_{23}, \zeta_{31}) \xrightarrow{\text{CFT}} \zeta_{31}^{-1+\gamma(4)} G(z, \bar{z}), \quad (3)$$

¹ We must also highlight the earlier work on energy correlators by Basham et al. [100–103], Konishi et al. [104], Tkachov et al. [84, 85, 105–107], and Korchemsky and Sterman [86, 108, 109].

² For applications to the Sudakov region, see [118–123].

and exhibits a featureless power-law scaling governed by the twist-2 spin-4 anomalous dimension, $\gamma(4)$ [88, 96, 114, 129]. This behavior has been measured [128] using publicly released CMS data [130, 131]. The functional form of $G(z, \bar{z})$ can be found in [115, 117].

In contrast, the top quark mass explicitly breaks the rescaling symmetry of the collinear limit. Thus m_t appears as a characteristic scale imprinted in the three-point correlator. While the top quark has a three-body decay at leading order, higher-order corrections give rise to additional radiation, which is primarily collinear to the decay products leading to a growth in the distribution at angles $\hat{\zeta}_{ij} \ll m_t^2/p_T^2$. To extract m_t , we therefore focus on the correlator in a specific energy flow configuration sensitive to the hard decay kinematics. In this *Letter* we study the simplest configuration, that of an equilateral triangle $\hat{\zeta}_{ij} = \zeta$ allowing for a small asymmetry ($\delta\zeta$). Thus the key object of our analysis is the n th energy weighted cross section

$$\frac{d\Sigma(\delta\zeta)}{dQd\zeta} = \int d\zeta_{12}d\zeta_{23}d\zeta_{31} \int d\sigma \widehat{\mathcal{M}}_{\Delta}^{(n)}(\zeta_{12}, \zeta_{23}, \zeta_{31}, \zeta, \delta\zeta), \quad (4)$$

where the measurement operator $\widehat{\mathcal{M}}_{\Delta}^{(n)}$ is

$$\begin{aligned} \widehat{\mathcal{M}}_{\Delta}^{(n)}(\zeta_{12}, \zeta_{23}, \zeta_{31}, \zeta, \delta\zeta) &= \widehat{\mathcal{M}}^{(n)}(\zeta_{12}, \zeta_{23}, \zeta_{31}) \\ &\times \delta(3\zeta - \zeta_{12} - \zeta_{23} - \zeta_{31}) \prod_{l,m,n \in \{1,2,3\}} \Theta(\delta\zeta - |\zeta_{lm} - \zeta_{mn}|). \end{aligned} \quad (5)$$

For $\delta\zeta \ll \zeta$,

$$\frac{d\Sigma}{d\zeta} \approx 4(\delta\zeta)^2 G^{(n)}(\zeta, \zeta, \zeta; m_t), \quad (6)$$

where we have made the dependence on m_t explicit. Three-body kinematics implies that the distribution is peaked at $\zeta_{\text{peak}} \approx 3m_t^2/Q^2$, exhibiting quadratic sensitivity to the top mass. At the LHC the peak is resilient to collinear radiation since $\ln \zeta_{\text{peak}} < 1/\alpha_s$, making its properties computable in fixed order perturbation theory at the hard scale. In the region $\zeta < 2\delta\zeta$ the hard three-body kinematics is no longer identified, leading to a bulge in the distribution (see the *Supplemental Material*). We leave optimization of $\delta\zeta$ for future work.

Mass Sensitivity in e^+e^- .—To illustrate the mass sensitivity of our observable, we begin with the simplest case of e^+e^- collisions. We simulate the $e^+e^- \rightarrow t + X$ process at a center of mass energy of $Q = 2000$ GeV using the PYTHIA8 parton shower [132]. We reconstruct anti- k_T [69] jets with $R = 1.2$ using FASTJET [71], and analyze them using the jet analysis software JETLIB [133]. Although jet clustering is not required in e^+e^- , this analysis strategy is chosen to achieve maximal similarity with the case of hadron colliders considered below.

In Fig. 2 we show the distribution of the three-point correlator in the peak region, both with and without the

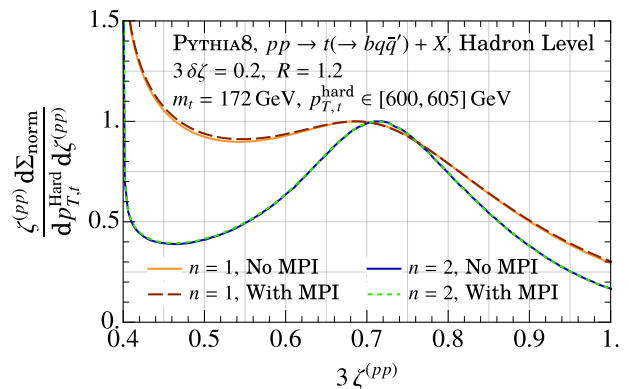


FIG. 3: The $n = 1, 2$ three-point correlators on decaying top quarks with a fixed hard p_T , with and without MPI. Here a clear peak can be seen at $\zeta \approx 3m_t^2/p_{T,t}^2$. No grooming has been applied.

effects of hadronization. Agreement of the peak position with the leading-order expectation is found, showing that the observed behavior is dictated by the hard decay of the top. In the top and bottom panels in Fig. 2, linear ($n = 1$) and quadratic ($n = 2$) energy weightings are used, see Eq. (2). The latter is not collinear safe, but for the energy correlators the collinear IR-divergences can be absorbed into moments of the fragmentation functions, as for track functions [83, 110].

Non-perturbative effects in energy correlators are governed by an additive underlying power law [86, 108, 109, 134], which over the width of the peak has a minimal effect on the normalized distribution. This is confirmed by the small differences in peak position between parton and hadron level distributions in Fig. 2. Taking $m_t = 170, 172$ GeV with $n = 2$ as representative distributions, we find that the shift due to hadronization corresponds to a $\Delta m_t^{\text{Had.}} \sim 250$ MeV shift in the top mass. This is in contrast with the groomed jet mass case where hadronization causes peak shifts equivalent to $\Delta m_t^{\text{Had.}} \sim 1$ GeV [77]. Zoomed in plots are shown in the *Supplemental Material*.

Hadron Colliders.—We now extend our discussion to the more challenging case of proton-proton collisions. This study illustrates, the difference between energy correlators and standard jet shape observables, and also emphasizes the irreducible difficulties of jet substructure at hadron colliders.

Implicit in the definition of energy correlators, $\langle \psi | \mathcal{E}(\vec{n}_1) \cdots \mathcal{E}(\vec{n}_k) | \psi \rangle$, is a characterization of the QCD final state $|\psi\rangle$ on which they are defined. In the case of e^+e^- collisions, the state can be defined by a local operator of definite momentum acting on the QCD vacuum, $|\psi\rangle = \mathcal{O}|0\rangle$, giving rise to a perfectly specified hard scale, Q . This is also the case considered in the CFT literature. In hadronic final states at proton-proton collisions, the states on which we compute the energy cor-

relators are necessarily defined through a measurement process on the hadronic radiation, e.g. by selecting anti- k_T jets with a specific $p_{T,\text{jet}}$. Due to the insensitivity of the energy correlators to soft radiation, we will show that it is in fact the non-perturbative effects on the jet p_T selection that are the source of complications in a hadron collider environment. This represents a significant advantage of our approach, since it shifts the standard problem of characterizing non-perturbative corrections to infrared jet shape observables, to characterizing non-perturbative effects on a *hard* scale. This enables us to propose a methodology for the precise extraction of m_t in hadron collisions by independently measuring the non-perturbative effects on the $p_{T,\text{jet}}$ spectrum. We now illustrate the key features of this approach.

The three-point correlator in hadron collisions is defined as

$$\widehat{\mathcal{M}}_{(pp)}^{(n)}(\zeta_{12}, \zeta_{23}, \zeta_{31}) = \sum_{i,j,k \in \text{jet}} \frac{(p_{T,i})^n (p_{T,j})^n (p_{T,k})^n}{(p_{T,\text{jet}})^{3n}} \times \delta\left(\zeta_{12} - \hat{\zeta}_{ij}^{(pp)}\right) \delta\left(\zeta_{23} - \hat{\zeta}_{ik}^{(pp)}\right) \delta\left(\zeta_{31} - \hat{\zeta}_{jk}^{(pp)}\right), \quad (7)$$

where $\hat{\zeta}_{ij}^{(pp)} = \Delta R_{ij}^2 = \sqrt{\Delta\eta_{ij}^2 + \Delta\phi_{ij}^2}$, with η, ϕ the standard rapidity, azimuth coordinates. Here the hard scale $p_{T,\text{jet}}$ appears, as opposed to Q in e^+e^- collisions, emphasizing that characterizing $p_{T,\text{jet}}$ will play a crucial role in our analysis. The peak of the EEEC distribution is determined by the hard kinematics and is found at $\zeta_{\text{peak}}^{(pp)} \approx 3m_t^2/p_{T,t}^2$, where $p_{T,t}$ is the top p_T , *not* $p_{T,\text{jet}}$.

To clearly illustrate the distinction between the infrared measurement of the EEEC and the hard measurement of the $p_{T,\text{jet}}$ spectrum, we present a two-step analysis using data generated in PYTHIA8. First, we generated hard top quark states with definite momentum (like in e^+e^-), but in the more complicated LHC environment including UE. This is shown in Fig. 3, where we see a clear peak that is *completely* independent of the presence of MPI (the PYTHIA8 model for UE), even without grooming. This illustrates that the correlators themselves, on a perfectly characterized top quark state, are insensitive to soft radiation, as in e^+e^- .

We then performed a proof-of-principles analysis to illustrate that a characterization of non-perturbative corrections to the $p_{T,\text{jet}}$ spectrum allows us to extract m_t , with small uncertainties from non-perturbative physics. While we will later give a factorization formula for the observable $d\Sigma(\delta\zeta)/dp_{T,\text{jet}} d\zeta$, for the present discussion it is useful to write it as

$$\frac{d\Sigma(\delta\zeta)}{dp_{T,\text{jet}} d\zeta} = \frac{d\Sigma(\delta\zeta)}{dp_{T,t} d\zeta} \frac{dp_{T,t}}{dp_{T,\text{jet}}}. \quad (8)$$

This formula, combined with Fig. 3, illustrates that the source of complications in the hadron-collider environment lies in the observable-independent function of *hard scales* $dp_{T,t}/dp_{T,\text{jet}}$, which receives both perturbative and

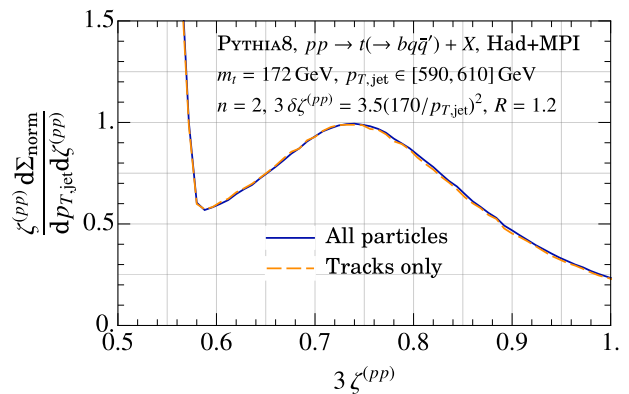


FIG. 4: The $n = 2$ three-point correlator on top jets in hadron collisions in a $p_{T,\text{jet}}$ window. A clear peak can be seen at $\zeta \approx 3m_t^2/p_{T,\text{jet}}^2$ which is insensitive to the usage of tracks.

non-perturbative contributions. To extract a value of the top quark mass, we write the peak position as

$$\zeta_{\text{peak}}^{(pp)} = \frac{3F_{\text{pert}}(m_t, p_{T,\text{jet}}, \alpha_s, R)}{(p_{T,\text{jet}} + \Delta_{\text{NP}}(R) + \Delta_{\text{MPI}}(R))^2}. \quad (9)$$

Here F_{pert} incorporates the effects of perturbative radiation. At leading order, $F_{\text{pert}} = m_t^2$. Corrections from hadronization and MPI are encoded through the shifts $\Delta_{\text{NP}}(R)$ and $\Delta_{\text{MPI}}(R)$. Crucially, in the factorization limit that we consider, these are not a property of the EEEC observable, but can instead be extracted directly from the non-perturbative corrections to the jet p_T spectrum [135]. This is a unique feature of our approach.

To illustrate the feasibility of this procedure, we used PYTHIA8 (including hadronization and MPI) to extract $\zeta_{\text{peak}}^{(pp)}$ as a function of $p_{T,\text{jet}}$, over an energy range within the expected reach of the high luminosity LHC. As a proxy for a perturbative calculation, we used parton level data to extract F_{pert} . To the accuracy we are working, F_{pert} is independent of the jet p_T , and can just be viewed as an effective top mass $\sqrt{F_{\text{pert}}}(m_t)$. We also extract $\Delta_{\text{NP}}(R) + \Delta_{\text{MPI}}(R)$ independently from the $p_{T,\text{jet}}$ spectrum.

Using Eq. (9) we fit $\zeta_{\text{peak}}^{(pp)}$ as a function of $p_{T,\text{jet}}$ for an effective value of $F_{\text{pert}}(m_t)$. An example of the distribution in the peak region is shown in Fig. 4, which also highlights the insensitivity of the peak position to the use of charged particles only (tracks). A fit to $\zeta_{\text{peak}}^{(pp)}$ for several $p_{T,\text{jet}}$ bins is shown in Fig. 5. With a perfect characterization of the non-perturbative corrections to the EEEC observable, the value of $F_{\text{pert}}(m_t)$ extracted when hadronization and MPI are included should exactly match its extraction at parton level. This would lead to complete control over m_t . In Table I we show the extracted value of $F_{\text{pert}}(m_t)$ from our parton level fit, and from our hadron+MPI level fit for two values of the

Pythia8 m_t . The errors quoted are the statistical errors on the parton shower analysis. The Hadron+MPI m_t is quoted with two errors: the first originates from the statistical error on the EEEC measurement, the second originates from the statistical error on the determination of $N_{\text{NP}}(R) + N_{\text{MPI}}(R)$ from the $p_{\text{T};\text{jet}}$ spectrum. A more detailed discussion of this procedure can be found in the Supplemental Material. Thus we find promising evidence that complete theoretical control of the top mass, up to errors $\sim 1\text{ GeV}$, is possible with an EEEC-based measurement. Our analysis also emphasizes the importance of understanding non-perturbative corrections to the jet p_{T} spectrum.

The goal of this Letter has been to introduce our novel approach to top mass measurements and illustrate its feasibility. This proof-of-principles analysis has shown that our approach overcomes many of the standard issues of jet shape based extractions. Nevertheless, there remain many areas in which our methodology could be improved to achieve greater statistical power and to bring it closer to experimental reality. These include the optimization of α_s , the binning of $p_{\text{T};\text{jet}}$ and $\langle p_{\text{T}} \rangle$, and including other shapes on the EEEC correlator. On the theoretical side, our promising results motivate developing a deeper understanding of the three-point correlator of boosted tops in the hadron collider environment.

Factorization Theorem. A key feature of our approach is a rigorous factorization theorem, which allows us to separate universal non-perturbative effects from perturbatively calculable contributions. It combines factorization for massless energy correlators [136] with the bHQET treatment of the top quark near its mass shell [27, 28, 43, 77]. This allows for a separation of the dynamics at the scale of the hard production, the jet radius R , the angle θ , and the top width Γ_t . While factorization is generically violated for hadronic jet shapes (see [137] for a recent discussion), our framework is based on the rigorous factorization for single particle massive fragmentation [138{145]. Assuming $\Gamma_t \ll R$, we perform a matching at the perturbative scale of the jet radius, using the fragmenting jet formalism [146{148], which captures the jet algorithm dependence. The final jet function describing the collinear dynamics at the scale of μ is therefore free of any jet algorithm dependence.

Combining these ingredients, we expect to obtain the following factorized expression

$$\frac{d}{dp_{\text{T};\text{jet}} d\theta} = f_i f_j H_{ij}(z_J; p_{\text{T};t}) \frac{p_{\text{T};\text{jet}}}{z_J}; \quad J_{t|t}(z_J; z_h; R) J_{\text{EEEEC}}^{\text{[tracks]}}(n; z_h; \mu; m_t; \Gamma_t); \quad (10)$$

for the energy-weighted cross section differential in $p_{\text{T};\text{jet}}$, rapidity y , and θ . This can be used to compute $F_{\text{pert}}(m_t)$ in a systematically improvable fashion. Obvious dependencies, such as on factorization scales, have been suppressed for compactness. Here, $\hat{\sigma}_i$ are parton distribu-

FIG. 5: Plot of the peak position as a function of $p_{\text{T};\text{jet}}$, as used in our fitting procedure.

Pythia8 m_t	Parton F_{pert}	Hadron + MPI F_{pert}
172 GeV	1726 \pm 0.3 GeV	1723 \pm 0.2 \pm 0.4 GeV
173 GeV	1735 \pm 0.3 GeV	1736 \pm 0.2 \pm 0.4 GeV
173 \pm 172	0.9 \pm 0.4 GeV	1.3 \pm 0.6 GeV

TABLE I: Values of the effective parameter $F_{\text{pert}}(m_t)$ extracted at parton level, and hadron+MPI level. The consistency of the two approaches provides a measure of our uncertainty due to non-perturbative corrections.

tion functions, and $H_{ij}(z_J; p_{\text{T};t})$ is the hard function for inclusive massive fragmentation [149, 150], which is known for LHC processes at NNLO [151]. $J_{t|t}$ is the fragmenting jet function, which is known at NLO for anti- k_{T} jets [147, 148], but can be extended to NNLO using the approach of [152]. The convolutions over $H_{ij}(z_J; p_{\text{T};t})$ and $J_{t|t}$ alone determine the $p_{\text{T};\text{jet}}$ spectrum, independent of the EEEC measurement. Finally, J_{EEEEC} is the energy correlator jet function, which can be computed in a short-distance top mass scheme, and can include information from track or fragmentation functions. Around the top peak, J_{EEEEC} is almost entirely determined by perturbative physics. In the region of on-shell top, it can be matched onto a jet function defined in bHQET [27, 28, 39, 40, 77]. The functions in the factorization formula above exhibit standard DGLAP [153{155] evolution in the momentum fractions z_J and $z_h = p_{\text{T};\text{hadron}} = p_{\text{T};\text{jet}}$, and the $\hat{\sigma}_i$ denote standard fragmentation convolutions. A more detailed study of the structure of the factorization, and a calculation of J_{EEEEC} , will be provided in a future publication.

Conclusions. We have proposed a new paradigm for jet-substructure based measurements of the top quark mass at the LHC in a rigorous field theoretic setup. Instead of using standard jet shape observables, we have analyzed the three-point correlator of energy flow operators, and have illustrated a number of its remarkable

features. Our results support the possibility of achieving complete theoretical control over an observable with top mass sensitivity competitive with direct measurements.

Acknowledgements.—We are particularly grateful to G. Salam for insightful questions that led us to (hopefully) significantly improve our presentation. We also thank B. Nachman, M. Schwartz, I. Stewart and W. Waalewijn for feedback on the manuscript. We thank H. Chen, P. Komiske, K. Lee, Y. Li, F. Ringer, J. Thaler, A. Venkata, X.Y. Zhang and H.X. Zhu for many useful discussions and collaborations on related topics that significantly influenced the philosophy of this work. A.P. is grateful to M. Vos, M. LeBlanc, J. Roloff and J. Aparisi-Pozo for many helpful discussions about subtleties of the top mass extraction at the LHC. This work is supported in part by the GLUODYNAMICS project funded by the “P2IO LabEx (ANR-10-LABX-0038)” in the framework “Investissements d’Avenir” (ANR-11-IDEX-0003-01) managed by the Agence Nationale de la Recherche (ANR), France. I.M. is supported by startup funds from Yale University. A.P. is a member of the Lancaster-Manchester-Sheffield Consortium for Fundamental Physics, which is supported by the UK Science and Technology Facilities Council (STFC) under grant number ST/T001038/1.

-
- [1] G. Degrassi, S. Di Vita, J. Elias-Miro, J. R. Espinosa, G. F. Giudice, G. Isidori, and A. Strumia, *JHEP* **08**, 098 (2012), arXiv:1205.6497 [hep-ph].
- [2] D. Buttazzo, G. Degrassi, P. P. Giardino, G. F. Giudice, F. Sala, A. Salvio, and A. Strumia, *JHEP* **12**, 089 (2013), arXiv:1307.3536 [hep-ph].
- [3] A. Andreassen, W. Frost, and M. D. Schwartz, *Phys. Rev. Lett.* **113**, 241801 (2014), arXiv:1408.0292 [hep-ph].
- [4] M. Baak, M. Goebel, J. Haller, A. Hoecker, D. Kennedy, R. Kogler, K. Moenig, M. Schott, and J. Stelzer, *Eur. Phys. J. C* **72**, 2205 (2012), arXiv:1209.2716 [hep-ph].
- [5] M. Baak, J. Cúth, J. Haller, A. Hoecker, R. Kogler, K. Mönig, M. Schott, and J. Stelzer (Gfitter Group), *Eur. Phys. J. C* **74**, 3046 (2014), arXiv:1407.3792 [hep-ph].
- [6] G. F. Giudice and R. Rattazzi, *Nucl. Phys. B* **757**, 19 (2006), arXiv:hep-ph/0606105.
- [7] J. Khoury and O. Parrikar, *JCAP* **12**, 014 (2019), arXiv:1907.07693 [hep-th].
- [8] J. Khoury, *JCAP* **06**, 009 (2021), arXiv:1912.06706 [hep-th].
- [9] G. Kartvelishvili, J. Khoury, and A. Sharma, *JCAP* **02**, 028 (2021), arXiv:2003.12594 [hep-th].
- [10] G. F. Giudice, M. McCullough, and T. You, *JHEP* **10**, 093 (2021), arXiv:2105.08617 [hep-ph].
- [11] G. Aad *et al.* (ATLAS, CMS), *Phys. Rev. Lett.* **114**, 191803 (2015), arXiv:1503.07589 [hep-ex].
- [12] V. S. Fadin and V. A. Khoze, *JETP Lett.* **46**, 525 (1987).
- [13] V. S. Fadin and V. A. Khoze, *Sov. J. Nucl. Phys.* **48**, 309 (1988).
- [14] M. J. Strassler and M. E. Peskin, *Phys. Rev. D* **43**, 1500 (1991).
- [15] M. Beneke, *Phys. Lett. B* **434**, 115 (1998), arXiv:hep-ph/9804241.
- [16] M. Beneke, A. Signer, and V. A. Smirnov, *Phys. Lett. B* **454**, 137 (1999), arXiv:hep-ph/9903260.
- [17] A. H. Hoang, A. V. Manohar, I. W. Stewart, and T. Teubner, *Phys. Rev. Lett.* **86**, 1951 (2001), arXiv:hep-ph/0011254.
- [18] A. H. Hoang, A. V. Manohar, I. W. Stewart, and T. Teubner, *Phys. Rev. D* **65**, 014014 (2002), arXiv:hep-ph/0107144.
- [19] M. Beneke, Y. Kiyo, P. Marquard, A. Penin, J. Piclum, and M. Steinhauser, *Phys. Rev. Lett.* **115**, 192001 (2015), arXiv:1506.06864 [hep-ph].
- [20] (2014), arXiv:1407.2682 [hep-ex].
- [21] V. Khachatryan *et al.* (CMS), *Phys. Rev. D* **93**, 072004 (2016), arXiv:1509.04044 [hep-ex].
- [22] M. Aaboud *et al.* (ATLAS), *Phys. Lett. B* **761**, 350 (2016), arXiv:1606.02179 [hep-ex].
- [23] P. A. Zyla *et al.* (Particle Data Group), *PTEP* **2020**, 083C01 (2020).
- [24] A. H. Hoang and I. W. Stewart, *Nucl. Phys. B Proc. Suppl.* **185**, 220 (2008), arXiv:0808.0222 [hep-ph].
- [25] P. Nason, “The Top Mass in Hadronic Collisions,” in *From My Vast Repertoire: Guido Altarelli’s Legacy*, edited by A. Levy, S. Forte, and G. Ridolfi (2019) pp. 123–151, arXiv:1712.02796 [hep-ph].
- [26] A. H. Hoang, *Ann. Rev. Nucl. Part. Sci.* **70**, 225 (2020), arXiv:2004.12915 [hep-ph].
- [27] S. Fleming, A. H. Hoang, S. Mantry, and I. W. Stewart, *Phys. Rev. D* **77**, 114003 (2008), arXiv:0711.2079 [hep-ph].
- [28] S. Fleming, A. H. Hoang, S. Mantry, and I. W. Stewart, *Phys. Rev. D* **77**, 074010 (2008), arXiv:hep-ph/0703207.
- [29] C. W. Bauer and I. W. Stewart, *Phys. Lett.* **B516**, 134 (2001), hep-ph/0107001.
- [30] C. W. Bauer, S. Fleming, D. Pirjol, and I. W. Stewart, *Phys. Rev. D* **63**, 114020 (2001), hep-ph/0011336.
- [31] C. W. Bauer, D. Pirjol, and I. W. Stewart, *Phys. Rev. D* **65**, 054022 (2002), hep-ph/0109045.
- [32] C. W. Bauer, S. Fleming, D. Pirjol, I. Z. Rothstein, and I. W. Stewart, *Phys. Rev.* **D66**, 014017 (2002), arXiv:hep-ph/0202088 [hep-ph].
- [33] E. Eichten and B. R. Hill, *Phys. Lett. B* **234**, 511 (1990).
- [34] N. Isgur and M. B. Wise, *Phys. Lett. B* **232**, 113 (1989).
- [35] N. Isgur and M. B. Wise, *Phys. Lett. B* **237**, 527 (1990).
- [36] B. Grinstein, *Nucl. Phys. B* **339**, 253 (1990).
- [37] H. Georgi, *Phys. Lett. B* **240**, 447 (1990).
- [38] A. V. Manohar and M. B. Wise, *Heavy quark physics*, Vol. 10 (2000).
- [39] A. H. Hoang, A. Jain, I. Scimemi, and I. W. Stewart, *Phys. Rev. Lett.* **101**, 151602 (2008), arXiv:0803.4214 [hep-ph].
- [40] A. H. Hoang, A. Jain, I. Scimemi, and I. W. Stewart, *Phys. Rev. D* **82**, 011501 (2010), arXiv:0908.3189 [hep-ph].
- [41] A. H. Hoang, A. Jain, C. Lepenik, V. Mateu, M. Preisser, I. Scimemi, and I. W. Stewart, *JHEP* **04**, 003 (2018), arXiv:1704.01580 [hep-ph].
- [42] A. H. Hoang, A. Pathak, P. Pietrulewicz, and I. W. Stewart, *JHEP* **12**, 059 (2015), arXiv:1508.04137 [hep-ph].

- [43] B. Bachu, A. H. Hoang, V. Mateu, A. Pathak, and I. W. Stewart, *Phys. Rev. D* **104**, 014026 (2021), arXiv:2012.12304 [hep-ph].
- [44] M. Butenschoen, B. Dehnadi, A. H. Hoang, V. Mateu, M. Preisser, and I. W. Stewart, *Phys. Rev. Lett.* **117**, 232001 (2016), arXiv:1608.01318 [hep-ph].
- [45] A. H. Hoang, S. Plätzer, and D. Samitz, *JHEP* **10**, 200 (2018), arXiv:1807.06617 [hep-ph].
- [46] ATLAS, ATLAS-PHYS-PUB-2021-034 (2021).
- [47] S. Höche, F. Krauss, and S. Prestel, *JHEP* **10**, 093 (2017), arXiv:1705.00982 [hep-ph].
- [48] S. Höche and S. Prestel, *Phys. Rev. D* **96**, 074017 (2017), arXiv:1705.00742 [hep-ph].
- [49] F. Dulat, S. Höche, and S. Prestel, *Phys. Rev. D* **98**, 074013 (2018), arXiv:1805.03757 [hep-ph].
- [50] M. Dasgupta, F. A. Dreyer, K. Hamilton, P. F. Monni, G. P. Salam, and G. Soyez, *Phys. Rev. Lett.* **125**, 052002 (2020), arXiv:2002.11114 [hep-ph].
- [51] J. R. Forshaw, J. Holguin, and S. Plätzer, *JHEP* **09**, 014 (2020), arXiv:2003.06400 [hep-ph].
- [52] A. Karlberg, G. P. Salam, L. Scyboz, and R. Verheyen, *Eur. Phys. J. C* **81**, 681 (2021), arXiv:2103.16526 [hep-ph].
- [53] K. Hamilton, R. Medves, G. P. Salam, L. Scyboz, and G. Soyez, (2020), 10.1007/JHEP03(2021)041, arXiv:2011.10054 [hep-ph].
- [54] J. Holguin, J. R. Forshaw, and S. Plätzer, *Eur. Phys. J. C* **81**, 364 (2021), arXiv:2011.15087 [hep-ph].
- [55] Z. Nagy and D. E. Soper, *Phys. Rev. D* **104**, 054049 (2021), arXiv:2011.04773 [hep-ph].
- [56] H. Brooks, C. T. Preuss, and P. Skands, *JHEP* **07**, 032 (2020), arXiv:2003.00702 [hep-ph].
- [57] K. Hamilton, A. Karlberg, G. P. Salam, L. Scyboz, and R. Verheyen, (2021), arXiv:2111.01161 [hep-ph].
- [58] G. Bewick, S. Ferrario Ravasio, P. Richardson, and M. H. Seymour, (2021), arXiv:2107.04051 [hep-ph].
- [59] L. Gellersen, S. Höche, and S. Prestel, (2021), arXiv:2110.05964 [hep-ph].
- [60] J. R. Forshaw, J. Holguin, and S. Plätzer, (2021), arXiv:2112.13124 [hep-ph].
- [61] R. Frederix and S. Frixione, *JHEP* **12**, 061 (2012), arXiv:1209.6215 [hep-ph].
- [62] S. Hoeche, F. Krauss, P. Maierhofer, S. Pozzorini, M. Schonherr, and F. Siegert, *Phys. Lett. B* **748**, 74 (2015), arXiv:1402.6293 [hep-ph].
- [63] T. Ježo, J. M. Lindert, P. Nason, C. Oleari, and S. Pozzorini, *Eur. Phys. J. C* **76**, 691 (2016), arXiv:1607.04538 [hep-ph].
- [64] R. Frederix, S. Frixione, A. S. Papanastasiou, S. Prestel, and P. Torrielli, *JHEP* **06**, 027 (2016), arXiv:1603.01178 [hep-ph].
- [65] K. Cormier, S. Plätzer, C. Reuschle, P. Richardson, and S. Webster, *Eur. Phys. J. C* **79**, 915 (2019), arXiv:1810.06493 [hep-ph].
- [66] J. Mazzitelli, P. F. Monni, P. Nason, E. Re, M. Wiesemann, and G. Zanderighi, *Phys. Rev. Lett.* **127**, 062001 (2021), arXiv:2012.14267 [hep-ph].
- [67] M. Cacciari and G. P. Salam, *Phys. Lett. B* **641**, 57 (2006), arXiv:hep-ph/0512210.
- [68] G. P. Salam and G. Soyez, *JHEP* **05**, 086 (2007), arXiv:0704.0292 [hep-ph].
- [69] M. Cacciari, G. P. Salam, and G. Soyez, *JHEP* **04**, 063 (2008), arXiv:0802.1189 [hep-ph].
- [70] G. P. Salam, *Eur. Phys. J. C* **67**, 637 (2010), arXiv:0906.1833 [hep-ph].
- [71] M. Cacciari, G. P. Salam, and G. Soyez, *Eur. Phys. J. C* **72**, 1896 (2012), arXiv:1111.6097 [hep-ph].
- [72] J. M. Butterworth, A. R. Davison, M. Rubin, and G. P. Salam, *Phys. Rev. Lett.* **100**, 242001 (2008), arXiv:0802.2470 [hep-ph].
- [73] D. E. Kaplan, K. Rehermann, M. D. Schwartz, and B. Tweedie, *Phys. Rev. Lett.* **101**, 142001 (2008), arXiv:0806.0848 [hep-ph].
- [74] D. Krohn, J. Thaler, and L.-T. Wang, *JHEP* **02**, 084 (2010), arXiv:0912.1342 [hep-ph].
- [75] A. J. Larkoski, I. Moult, and B. Nachman, *Phys. Rept.* **841**, 1 (2020), arXiv:1709.04464 [hep-ph].
- [76] S. Marzani, G. Soyez, and M. Spannowsky, *Looking inside jets: an introduction to jet substructure and boosted-object phenomenology*, Vol. 958 (Springer, 2019) arXiv:1901.10342 [hep-ph].
- [77] A. H. Hoang, S. Mantry, A. Pathak, and I. W. Stewart, *Phys. Rev. D* **100**, 074021 (2019), arXiv:1708.02586 [hep-ph].
- [78] M. Dasgupta, A. Fregoso, S. Marzani, and G. P. Salam, *JHEP* **09**, 029 (2013), arXiv:1307.0007 [hep-ph].
- [79] A. J. Larkoski, S. Marzani, G. Soyez, and J. Thaler, *JHEP* **05**, 146 (2014), arXiv:1402.2657 [hep-ph].
- [80] A. M. Sirunyan *et al.* (CMS), *Eur. Phys. J. C* **77**, 467 (2017).
- [81] CMS, CMS-PAS-TOP-19-005 (2019).
- [82] A. H. Hoang, S. Mantry, A. Pathak, and I. W. Stewart, *JHEP* **12**, 002 (2019), arXiv:1906.11843 [hep-ph].
- [83] H. Chen, I. Moult, X. Zhang, and H. X. Zhu, *Phys. Rev. D* **102**, 054012 (2020), arXiv:2004.11381 [hep-ph].
- [84] N. Sveshnikov and F. Tkachov, *Phys. Lett. B* **382**, 403 (1996), arXiv:hep-ph/9512370.
- [85] F. V. Tkachov, *Int. J. Mod. Phys. A* **12**, 5411 (1997), arXiv:hep-ph/9601308.
- [86] G. P. Korchemsky and G. F. Sterman, *Nucl. Phys. B* **555**, 335 (1999), arXiv:hep-ph/9902341.
- [87] C. W. Bauer, S. P. Fleming, C. Lee, and G. F. Sterman, *Phys. Rev. D* **78**, 034027 (2008), arXiv:0801.4569 [hep-ph].
- [88] D. M. Hofman and J. Maldacena, *JHEP* **05**, 012 (2008), arXiv:0803.1467 [hep-th].
- [89] A. Belitsky, S. Hohenegger, G. Korchemsky, E. Sokatchev, and A. Zhiboedov, *Nucl. Phys. B* **884**, 305 (2014), arXiv:1309.0769 [hep-th].
- [90] A. Belitsky, S. Hohenegger, G. Korchemsky, E. Sokatchev, and A. Zhiboedov, *Nucl. Phys. B* **884**, 206 (2014), arXiv:1309.1424 [hep-th].
- [91] P. Kravchuk and D. Simmons-Duffin, *JHEP* **11**, 102 (2018), arXiv:1805.00098 [hep-th].
- [92] A. Belitsky, S. Hohenegger, G. Korchemsky, E. Sokatchev, and A. Zhiboedov, *Phys. Rev. Lett.* **112**, 071601 (2014), arXiv:1311.6800 [hep-th].
- [93] A. Belitsky, S. Hohenegger, G. Korchemsky, and E. Sokatchev, *Nucl. Phys. B* **904**, 176 (2016), arXiv:1409.2502 [hep-th].
- [94] G. Korchemsky and E. Sokatchev, *JHEP* **12**, 133 (2015), arXiv:1504.07904 [hep-th].
- [95] M. Kologlu, P. Kravchuk, D. Simmons-Duffin, and A. Zhiboedov, (2019), arXiv:1904.05905 [hep-th].
- [96] M. Kologlu, P. Kravchuk, D. Simmons-Duffin, and A. Zhiboedov, (2019), arXiv:1905.01311 [hep-th].
- [97] C.-H. Chang, M. Kologlu, P. Kravchuk, D. Simmons-Duffin, and A. Zhiboedov, (2020), arXiv:2010.04726

- [hep-th].
- [98] G. Korchemsky, E. Sokatchev, and A. Zhiboedov, (2021), arXiv:2106.14899 [hep-th].
- [99] G. P. Korchemsky and A. Zhiboedov, (2021), arXiv:2109.13269 [hep-th].
- [100] C. Basham, L. S. Brown, S. D. Ellis, and S. T. Love, Phys. Rev. Lett. **41**, 1585 (1978).
- [101] C. L. Basham, L. S. Brown, S. D. Ellis, and S. T. Love, Phys. Rev. D **17**, 2298 (1978).
- [102] C. L. Basham, L. S. Brown, S. D. Ellis, and S. T. Love, Phys. Lett. B **85**, 297 (1979).
- [103] C. Basham, L. Brown, S. Ellis, and S. Love, Phys. Rev. D **19**, 2018 (1979).
- [104] K. Konishi, A. Ukawa, and G. Veneziano, Nucl. Phys. **B157**, 45 (1979).
- [105] F. V. Tkachov, Phys. Rev. Lett. **73**, 2405 (1994), arXiv:hep-ph/9901332.
- [106] F. V. Tkachov, Int. J. Mod. Phys. A **17**, 2783 (2002), arXiv:hep-ph/9901444.
- [107] D. Y. Grigoriev, E. Jankowski, and F. V. Tkachov, Phys. Rev. Lett. **91**, 061801 (2003), arXiv:hep-ph/0301185.
- [108] G. P. Korchemsky and G. F. Sterman, Nucl. Phys. B **437**, 415 (1995), arXiv:hep-ph/9411211.
- [109] G. P. Korchemsky, G. Oderda, and G. F. Sterman, AIP Conf. Proc. **407**, 988 (1997), arXiv:hep-ph/9708346.
- [110] Y. Li, I. Moulton, S. S. van Velzen, W. J. Waalewijn, and H. X. Zhu, (2021), arXiv:2108.01674 [hep-ph].
- [111] M. Jaarsma, Y. Li, I. Moulton, W. Waalewijn, and H. X. Zhu, (2022), arXiv:2201.05166 [hep-ph].
- [112] H.-M. Chang, M. Procura, J. Thaler, and W. J. Waalewijn, Phys. Rev. Lett. **111**, 102002 (2013), arXiv:1303.6637 [hep-ph].
- [113] H.-M. Chang, M. Procura, J. Thaler, and W. J. Waalewijn, Phys. Rev. **D88**, 034030 (2013), arXiv:1306.6630 [hep-ph].
- [114] L. J. Dixon, I. Moulton, and H. X. Zhu, Phys. Rev. D **100**, 014009 (2019), arXiv:1905.01310 [hep-ph].
- [115] H. Chen, M.-X. Luo, I. Moulton, T.-Z. Yang, X. Zhang, and H. X. Zhu, JHEP **08**, 028 (2020), arXiv:1912.11050 [hep-ph].
- [116] H. Chen, I. Moulton, and H. X. Zhu, (2020), arXiv:2011.02492 [hep-ph].
- [117] H. Chen, I. Moulton, and H. X. Zhu, (2021), arXiv:2104.00009 [hep-ph].
- [118] I. Moulton and H. X. Zhu, JHEP **08**, 160 (2018), arXiv:1801.02627 [hep-ph].
- [119] I. Moulton, G. Vita, and K. Yan, JHEP **07**, 005 (2020), arXiv:1912.02188 [hep-ph].
- [120] A. Gao, H. T. Li, I. Moulton, and H. X. Zhu, Phys. Rev. Lett. **123**, 062001 (2019), arXiv:1901.04497 [hep-ph].
- [121] M. A. Ebert, B. Mistlberger, and G. Vita, (2020), arXiv:2012.07859 [hep-ph].
- [122] H. T. Li, I. Vitev, and Y. J. Zhu, JHEP **11**, 051 (2020), arXiv:2006.02437 [hep-ph].
- [123] H. T. Li, Y. Makris, and I. Vitev, (2021), arXiv:2102.05669 [hep-ph].
- [124] L. J. Dixon, M.-X. Luo, V. Shtabovenko, T.-Z. Yang, and H. X. Zhu, Phys. Rev. Lett. **120**, 102001 (2018), arXiv:1801.03219 [hep-ph].
- [125] M.-X. Luo, V. Shtabovenko, T.-Z. Yang, and H. X. Zhu, JHEP **06**, 037 (2019), arXiv:1903.07277 [hep-ph].
- [126] J. Henn, E. Sokatchev, K. Yan, and A. Zhiboedov, Phys. Rev. D **100**, 036010 (2019), arXiv:1903.05314 [hep-th].
- [127] M. Jankowiak and A. J. Larkoski, JHEP **06**, 057 (2011), arXiv:1104.1646 [hep-ph].
- [128] P. T. Komiske, I. Moulton, J. Thaler, and H. X. Zhu, .
- [129] G. Korchemsky, JHEP **01**, 008 (2020), arXiv:1905.01444 [hep-th].
- [130] S. Chatrchyan *et al.* (CMS), JINST **3**, S08004 (2008).
- [131] P. T. Komiske, R. Mastandrea, E. M. Metodiev, P. Naik, and J. Thaler, Phys. Rev. D **101**, 034009 (2020), arXiv:1908.08542 [hep-ph].
- [132] T. Sjöstrand, S. Ask, J. R. Christiansen, R. Corke, N. Desai, P. Ilten, S. Mrenna, S. Prestel, C. O. Rasmussen, and P. Z. Skands, Comput. Phys. Commun. **191**, 159 (2015), arXiv:1410.3012 [hep-ph].
- [133] A. E. Ferdinand, A. Pathak, *et al.*, (to be made public) (2019).
- [134] A. V. Belitsky, G. P. Korchemsky, and G. F. Sterman, Phys. Lett. B **515**, 297 (2001), arXiv:hep-ph/0106308.
- [135] M. Dasgupta, L. Magnea, and G. P. Salam, JHEP **02**, 055 (2008), arXiv:0712.3014 [hep-ph].
- [136] I. Moulton, F. Ringer, and H. X. Zhu, .
- [137] J. R. Forshaw and J. Holguin, (2021), arXiv:2109.03665 [hep-ph].
- [138] J. C. Collins and G. F. Sterman, Nucl. Phys. B **185**, 172 (1981).
- [139] G. T. Bodwin, Phys. Rev. D **31**, 2616 (1985), [Erratum: Phys.Rev.D 34, 3932 (1986)].
- [140] J. C. Collins, D. E. Soper, and G. F. Sterman, Nucl. Phys. B **261**, 104 (1985).
- [141] J. C. Collins, D. E. Soper, and G. F. Sterman, Nucl. Phys. B **308**, 833 (1988).
- [142] J. C. Collins, D. E. Soper, and G. F. Sterman, Adv. Ser. Direct. High Energy Phys. **5**, 1 (1989), arXiv:hep-ph/0409313.
- [143] J. Collins, *Foundations of perturbative QCD*, Vol. 32 (Cambridge University Press, 2013).
- [144] G. C. Nayak, J.-W. Qiu, and G. F. Sterman, Phys. Rev. D **72**, 114012 (2005), arXiv:hep-ph/0509021.
- [145] A. Mitov and G. Sterman, Phys. Rev. D **86**, 114038 (2012), arXiv:1209.5798 [hep-ph].
- [146] M. Procura and I. W. Stewart, Phys. Rev. D **81**, 074009 (2010), [Erratum: Phys.Rev.D 83, 039902 (2011)], arXiv:0911.4980 [hep-ph].
- [147] Z.-B. Kang, F. Ringer, and I. Vitev, JHEP **10**, 125 (2016), arXiv:1606.06732 [hep-ph].
- [148] Z.-B. Kang, F. Ringer, and I. Vitev, JHEP **11**, 155 (2016), arXiv:1606.07063 [hep-ph].
- [149] B. Mele and P. Nason, Phys. Lett. B **245**, 635 (1990).
- [150] B. Mele and P. Nason, Nucl. Phys. B **361**, 626 (1991), [Erratum: Nucl.Phys.B 921, 841–842 (2017)].
- [151] M. L. Czakon, T. Generet, A. Mitov, and R. Poncet, (2021), arXiv:2102.08267 [hep-ph].
- [152] H.-y. Liu, X. Liu, and S.-O. Moch, Phys. Rev. D **104**, 014016 (2021), arXiv:2103.08680 [hep-ph].
- [153] Y. L. Dokshitzer, Sov. Phys. JETP **46**, 641 (1977).
- [154] V. N. Gribov and L. N. Lipatov, Sov. J. Nucl. Phys. **15**, 438 (1972).
- [155] G. Altarelli and G. Parisi, Nucl. Phys. B **126**, 298 (1977).

Supplemental Material to A New Paradigm for Precision Top Physics: Weighing the Top with Energy Correlators

Jack Holguin, Ian Moulton, Aditya Pathak, Massimiliano Procura

Details of the EEEC Observable Definition

In this *Supplemental Material* we will provide a more detailed discussion of the leading-order analysis of the observable we have presented in the main text and of the effect of the smearing $\delta\zeta$. For concreteness, we will define the kinematics assuming a $e^+e^- \rightarrow t(\rightarrow bq\bar{q}') + X$ process where we take the b, q, \bar{q}' partons to be massless. No further complications, beyond the need for more ink, are introduced by using the longitudinally invariant kinematics needed for measurements at the LHC.

The starting point of our analysis is the normalized (energy weighted) differential cross section given by

$$\frac{1}{\sigma} \frac{d\Sigma}{dQ d\zeta_{12} d\zeta_{23} d\zeta_{31}} = \frac{1}{\sigma} \int \frac{d\sigma}{dQ} \widehat{\mathcal{M}}^{(n)}(\zeta_{12}, \zeta_{23}, \zeta_{31}), \quad (11)$$

where $\widehat{\mathcal{M}}^{(n)}$ denotes the measurement function as defined in Eq. (2).

At leading order, we can factorize the Born cross-section $d\sigma^{(0)}/\sigma^{(0)}$ into the dimensionless three-body phase space for the top's decay products, $d\Phi_3$, and the dimensionless weighted squared matrix element, $\sigma_t |M(t \rightarrow bW \rightarrow bq\bar{q}')|^2/\sigma^{(0)}$ where σ_t is the cross section to produce a top quark. As $|M(t \rightarrow bW \rightarrow bq\bar{q}')|^2 \sim \mathcal{O}(1)$, we can further approximate the EEEC distribution as

$$\frac{1}{\sigma^{(0)}} \frac{d\Sigma^{(0)}}{dQ d\zeta_{12} d\zeta_{23} d\zeta_{31}} \approx \int d\Phi_3 \widehat{\mathcal{M}}^{(n)}(\zeta_{12}, \zeta_{23}, \zeta_{31}), \quad (12)$$

reducing the problem of understanding the observable of interest to studying three-body kinematics.

Before directly working with Eq. (12), let us develop some intuition for the three-body kinematics. Consider the decay of a top quark in its rest frame, with $\tilde{p}_t = \tilde{p}_b + \tilde{p}_q + \tilde{p}_{\bar{q}'}$. Here we are using \tilde{p}_i as a rest-frame momentum and p_i as a lab-frame momentum. In the top rest frame, the angular parameters on which the EEEC depends are given by

$$\tilde{\zeta}_{12} = \frac{\tilde{p}_b \cdot \tilde{p}_q}{2\tilde{E}_b \tilde{E}_q}, \quad \tilde{\zeta}_{31} = \frac{\tilde{p}_b \cdot \tilde{p}_{\bar{q}'}}{2\tilde{E}_b \tilde{E}_{\bar{q}'}}}, \quad \tilde{\zeta}_{23} = \frac{\tilde{p}_q \cdot \tilde{p}_{\bar{q}'}}{2\tilde{E}_q \tilde{E}_{\bar{q}'}}}. \quad (13)$$

Momentum conservation requires that $\tilde{\zeta}_{12} + \tilde{\zeta}_{23} + \tilde{\zeta}_{31} \in [2, 2.25]$. Let the lab frame top momentum be $p_t = (E_t, \vec{p}_t)$. In the boost between the lab and rest frame, $\cosh \beta = E_t/m_t \sim \zeta^{-1/2}$. To first order in $m_t/E_t \ll 1$, we also have $\sinh \beta \approx \cosh \beta$. Hence the sum of lab frame EEEC parameters is

$$\zeta_{12} + \zeta_{23} + \zeta_{31} \approx \left(\frac{m_t}{E_t}\right)^2 \left(\tilde{x}_{tb}\tilde{x}_{tq}\tilde{\zeta}_{12} + \tilde{x}_{tb}\tilde{x}_{t\bar{q}'}\tilde{\zeta}_{31} + \tilde{x}_{tq}\tilde{x}_{t\bar{q}'}\tilde{\zeta}_{23}\right), \quad (14)$$

where

$$\tilde{x}_{ti} = (1 + \cos \tilde{\theta}_{ti}), \quad (15)$$

with $\tilde{\theta}_{ti}$ denoting the angle between parton i and the boost axis in the top's rest frame. The function

$$g \equiv \tilde{x}_{tb}\tilde{x}_{tq}\tilde{\zeta}_{12} + \tilde{x}_{tb}\tilde{x}_{t\bar{q}'}\tilde{\zeta}_{31} + \tilde{x}_{tq}\tilde{x}_{t\bar{q}'}\tilde{\zeta}_{23}$$

is also kinematically bounded so that $g \in [0, 3]$. Upon averaging over the possible boost axes one finds that $\langle g \rangle \in [1, 2.25]$. Thus, returning to Eq. (12), we expect the partially integrated EEEC distribution

$$\frac{d\Sigma}{dQ d\zeta} = \int d\zeta_{12} d\zeta_{23} d\zeta_{31} \times \frac{d\Sigma^{(0)}}{dQ d\zeta_{12} d\zeta_{23} d\zeta_{31}} \delta(3\zeta - \zeta_{12} - \zeta_{23} - \zeta_{31}), \quad (16)$$

to be peaked around $\zeta \approx \langle g \rangle m_t^2/(3E_t^2) \approx 2m_t^2/(3E_t^2)$. However, this peak will have a large width (of the order of

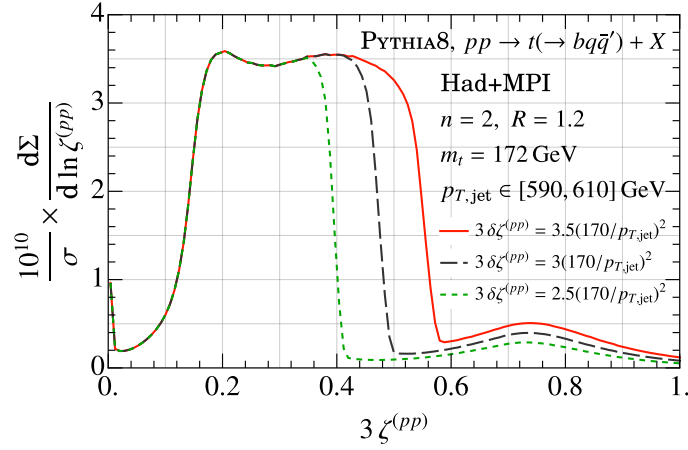


FIG. 6: The effect of applying different $\delta\zeta$ cuts to ensure an equilateral configuration in $pp \rightarrow t + X$. The $\delta\zeta$ cuts isolate the peak, which is governed by the hard decay of the top, from the “bulge” contribution.

$3m_t^2/(4E_t^2)$), whose origin can be understood by interpreting the parameters $\tilde{x}_{ti} \in [0, 2]$ as three sources of (correlated) random noise in the shape of the flow of energy which ‘smears’ the EEEC distribution. We can largely remove the noise by constraining the shape of the energy flow on the celestial sphere. This is most simply done by requiring that $\sqrt{\zeta_{ij}}$ approximately form the sides of an equilateral triangle ($\sqrt{\zeta_{ij}} \approx \sqrt{\zeta_{ik}}$). Consequently,

$$\tilde{x}_{tb}\tilde{x}_{tq}\tilde{\zeta}_{12} \approx \tilde{x}_{tb}\tilde{x}_{tq'}\tilde{\zeta}_{31} \approx \tilde{x}_{tq}\tilde{x}_{tq'}\tilde{\zeta}_{23}, \quad (17)$$

removing two of the noisy degrees of freedom from the distribution. Upon including this constraint, we find that $\langle g \rangle \approx 2.1$ with a small variance. This motivates us to introduce an EEEC distribution on equally spaced triplets of partons and allow for small asymmetries around this configuration governed by the parameter $\delta\zeta$:

$$\frac{d\Sigma(\delta\zeta)}{dQd\zeta} = \int d\zeta_{12}d\zeta_{23}d\zeta_{31} \int d\sigma \widehat{\mathcal{M}}_{\Delta}^{(n)}(\zeta_{12}, \zeta_{23}, \zeta_{31}, \zeta, \delta\zeta), \quad (18)$$

where the operator $\widehat{\mathcal{M}}_{\Delta}^{(n)}$ in the collinear limit is

$$\begin{aligned} \widehat{\mathcal{M}}_{\Delta}^{(n)}(\zeta_{12}, \zeta_{23}, \zeta_{31}, \zeta, \delta\zeta) &= \sum_{i,j,k} \frac{E_i^n E_j^n E_k^n}{Q^{3n}} \delta\left(\zeta_{12} - \frac{\theta_{ij}^2}{4}\right) \delta\left(\zeta_{31} - \frac{\theta_{ik}^2}{4}\right) \delta\left(\zeta_{23} - \frac{\theta_{jk}^2}{4}\right) \\ &\times \delta(3\zeta - \zeta_{12} - \zeta_{23} - \zeta_{31}) \prod_{l,m,n \in \{1,2,3\}} \Theta(\delta\zeta - |\zeta_{lm} - \zeta_{mn}|). \end{aligned}$$

As previously explained, three-body kinematics determines that this distribution is peaked at $\zeta_{\text{peak}} \approx 3m_t^2/(4E_t^2) \sim m_t^2/Q^2$. Furthermore, at the LHC the peak should be resilient to collinear radiation since $\ln \zeta_{\text{peak}} < 1/\alpha_s$.

We can now complete our leading-order discussion by computing the Born contribution to Eq. (18). Expanding for $\delta\zeta \ll \zeta$, we obtain

$$\begin{aligned} \frac{d\Sigma^0(\delta\zeta)}{dQd\zeta} &\propto (\delta\zeta)^2 \int_0^1 dz_1 dz_2 dz_3 \left(\frac{z_1 z_2 z_3}{8}\right)^n \times \delta\left(\frac{m_t^2}{4E_t^2} - z_1 z_2 \zeta - z_1 z_3 \zeta - z_2 z_3 \zeta\right) \\ &\times \delta(1 - z_1 - z_2 - z_3) |M(t \rightarrow bW \rightarrow bq\bar{q}')|^2, \end{aligned}$$

where $z_1 = E_b/E_t$ and $z_2 = E_{q'}/E_t$. The delta function causes the distribution to be sharply peaked at $\zeta = 3m_t^2/(4E_t^2)$. This matches the intuition we have developed from considering pure kinematics.

Looking at Eq. (18) to all orders in α_s :

$$\frac{d\Sigma(\delta\zeta)}{dQd\zeta} \approx 4(\delta\zeta)^2 G^{(n)}(\zeta, \zeta, \zeta) = \frac{d\Sigma^0(\delta\zeta)}{dQd\zeta} + \mathcal{O}(\alpha_s), \quad (19)$$

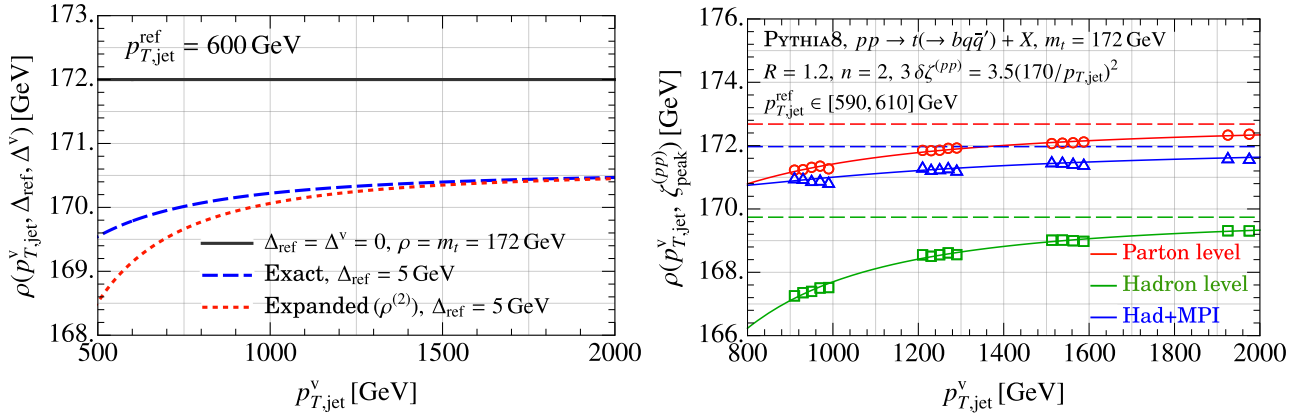


FIG. 7: On the left, we show the function ρ defined in the text for $\Delta^{\text{ref}} = 0$ GeV, as well as the exact and expanded to second order ($\rho^{(2)}$) for $\Delta^{\text{ref}} = 5$ GeV. On the right, we show an example of the best fit for ρ 's asymptote (ρ_{asy}) using the function $\rho = \rho_{\text{asy}} + c_2(p_{T,\text{jet}}^v)^{-2} + c_3(p_{T,\text{jet}}^v)^{-3}$. The data being fitted is produced using PYTHIA8 with $m_t = 172$ and with $p_{T,\text{jet}}^{\text{ref}}$ binned in the range $p_{T,\text{jet}}^{\text{ref}} \in [590, 610]$ GeV. The dashed lines are the best fit for the asymptotes, $\rho = \rho_{\text{asy}}$. No error bars are shown in this figure as it was produced from a single Monte Carlo sample. Fits of five samples are averaged over to produce the results and their errors in Table II.

to leading order in $\delta\zeta \ll \zeta$, whilst in the region where $2\delta\zeta > \zeta$

$$\frac{d\Sigma(\delta\zeta)}{dQd\zeta} \approx \int d\zeta_{12}d\zeta_{23}d\zeta_{31} G^{(n)}(\zeta_{12}, \zeta_{23}, \zeta_{31}). \quad (20)$$

Fig. 6 demonstrates that this dependence on $\delta\zeta$ is born out in simulation. To conclude our discussion of $\delta\zeta$, the limiting cases discussed above motivate that an optimal choice of this parameter will be a function of Q that strikes a balance between statistics and constraining the three-body kinematics ($\delta\zeta_{\text{optimal}} \approx \kappa \zeta_{\text{peak}}/2$ for $\kappa \lesssim 1$). A more sophisticated analysis may also sum over several shapes of energy flow on the celestial sphere to increase statistics — perhaps allowing for smaller values of $\delta\zeta_{\text{optimal}}$.

Details of the EEEEC Analysis at Proton-Proton Colliders

The longitudinally boost invariant measurement operator for the EEEEC observable is

$$\widehat{\mathcal{M}}_{(pp)}^{(n)}(\zeta_{12}, \zeta_{23}, \zeta_{31}) = \sum_{i,j,k \in \text{jet}} \frac{(p_{T,i})^n (p_{T,j})^n (p_{T,k})^n}{(p_{T,\text{jet}})^{3n}} \delta(\zeta_{12} - \hat{\zeta}_{ij}^{(pp)}) \delta(\zeta_{23} - \hat{\zeta}_{ik}^{(pp)}) \delta(\zeta_{31} - \hat{\zeta}_{jk}^{(pp)}), \quad (21)$$

where $\hat{\zeta}_{ij}^{(pp)} = \Delta R_{ij}^2 = \sqrt{\Delta\eta_{ij}^2 + \Delta\phi_{ij}^2}$. As before, the peak of the $\widehat{\mathcal{M}}_{\Delta}^{(n)}$ EEEEC distribution is determined by the top quark hard kinematics and is found at $\zeta_{\text{peak}}^{(pp)} \approx 3m_t^2/p_{T,t}^2$, where $p_{T,t}$ is the hard top p_T , *not* $p_{T,\text{jet}}$. Consequently, the basic properties of the $d\Sigma(\delta\zeta)/dp_{T,t} d\zeta$ distribution are completely insensitive to non-perturbative physics. In the previous section we demonstrated this insensitivity by parton shower simulation wherein we showed evidence that the top decay peak is nearly entirely independent of hadronization and UE. Consequently, in the limit that $p_{T,t}/(\Delta_{\text{NP}} + \Delta_{\text{MPI}}) \rightarrow \infty$, the top decay peak position is exactly independent of non-perturbative effects. However, since $p_{T,t}$ is not directly accessible, the observable we consider is

$$\frac{d\Sigma(\delta\zeta)}{dp_{T,\text{jet}} d\zeta} = \frac{d\Sigma(\delta\zeta)}{dp_{T,t} d\zeta} \frac{dp_{T,t}}{dp_{T,\text{jet}}}, \quad (22)$$

where $p_{T,\text{jet}}$ is the p_T of an identified anti- k_T top-jet. The top peak position in the distribution $d\Sigma(\delta\zeta)/dp_{T,\text{jet}} d\zeta$ will be shifted by hadronization and UE due to shifts in the jet p_T distribution. This shift can be measured independently from our observable and will be universal to all measurements of energy correlators on top quarks at the LHC.

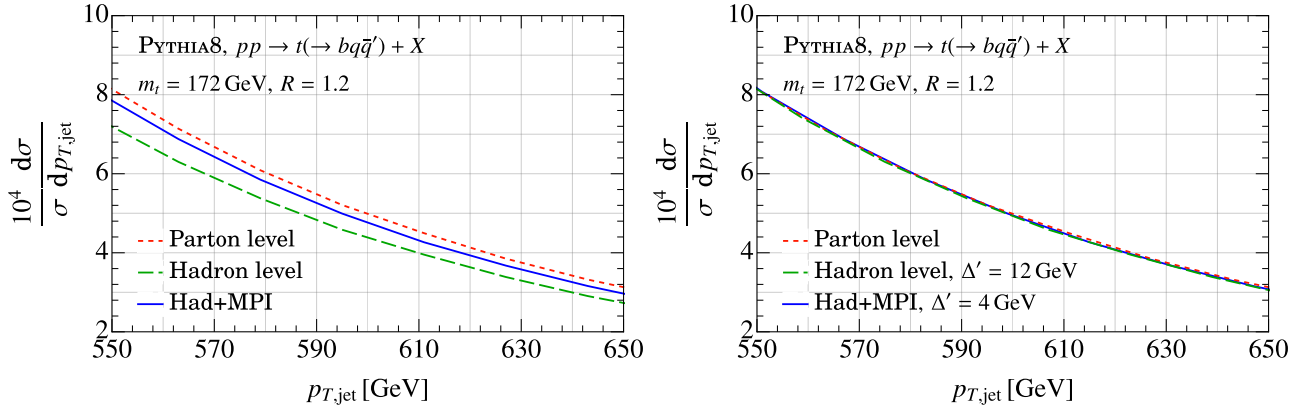


FIG. 8: On the left, the $p_{T,\text{jet}}$ spectrum at parton level, hadron level, and including MPI. A precise characterization of the states on which the energy correlator is computed requires an understanding of the non-perturbative shifts between these distributions. On the right, the hadron level and hadron+MPI curves shifted by constant values so that the three curves overlap. In both figures $p_{T,\text{jet}} \in [550, 650]$ GeV as this is the range in which we chose $p_{T,\text{jet}}^{\text{ref}}$ in our analysis.

We can parameterize the all-orders peak position in $d\Sigma(\delta\zeta)/dp_{T,\text{jet}} d\zeta$ as

$$\zeta_{\text{peak}}^{(pp)} = 3(1 + \mathcal{O}(\alpha_s)) \frac{m_t^2}{f(p_{T,\text{jet}}, m_t, \alpha_s, \Lambda_{\text{QCD}})^2} \equiv 3(1 + \mathcal{O}(\alpha_s)) \frac{m_t^2}{(p_{T,\text{jet}} + \Delta(p_{T,\text{jet}}, m_t, \alpha_s, \Lambda_{\text{QCD}}))^2}. \quad (23)$$

Mainly, Δ receives three additive contributions from perturbative radiation, hadronization, and from UE/MPI:

$$\Delta = \Delta_{\text{pert}} + \Delta_{\text{NP}} + \Delta_{\text{MPI}}. \quad (24)$$

Some simple manipulations can be made so as to minimize the sensitivity to Δ in an extracted value of m_t . We define the following function of measurable and perturbatively calculable quantities,

$$\rho^2(\zeta_{\text{peak}}^{(pp)v}, p_{T,\text{jet}}^v) = \left(\zeta_{\text{peak}}^{(pp)\text{ref}} - \zeta_{\text{peak}}^{(pp)v} \right) \left(\frac{3(1 + \mathcal{O}(\alpha_s))}{(p_{T,\text{jet}}^v)^2} - \frac{3(1 + \mathcal{O}(\alpha_s))}{(p_{T,\text{jet}}^{\text{ref}})^2} \right)^{-1}, \quad (25)$$

where $\zeta_{\text{peak}}^{(pp)\text{ref}}$ is the peak position in a fixed reference p_T bin, $p_{T,\text{jet}}^{\text{ref}}$, and $\zeta_{\text{peak}}^{(pp)v}$ is the peak position for a variable $p_{T,\text{jet}}$ value, $p_{T,\text{jet}}^v$, larger than the reference value (we require $p_{T,\text{jet}}^v > p_{T,\text{jet}}^{\text{ref}}$ to avoid divergences). ρ^2 is defined so that, in the limit $p_{T,\text{jet}}^v, p_{T,\text{jet}}^{\text{ref}} \rightarrow \infty$, we have $\rho^2 \rightarrow m_t^2$. In the analysis below we set $3(1 + \mathcal{O}(\alpha_s)) \mapsto 3$ so that, in the limit $p_{T,\text{jet}}^v, p_{T,\text{jet}}^{\text{ref}} \rightarrow \infty$, we find $\rho^2 \rightarrow F_{\text{pert}}$ as defined in the main body of this *Letter*. Now let us make a further definition,

$$\Delta^{\text{ref}} \equiv \Delta(p_{T,\text{jet}}^{\text{ref}}, m_t, \alpha_s, \Lambda_{\text{QCD}}), \quad \Delta^v(p_{T,\text{jet}}^v - p_{T,\text{jet}}^{\text{ref}}, m_t, \alpha_s, \Lambda_{\text{QCD}}) \equiv \Delta(p_{T,\text{jet}}^v, m_t, \alpha_s, \Lambda_{\text{QCD}}) - \Delta^{\text{ref}}. \quad (26)$$

We can substitute Eq. (23) into Eq. (25) to find $\rho(p_{T,\text{jet}}^v, \Delta^{\text{ref}}, \Delta^v)$, which is plotted in Fig. 7, left.

ρ has an asymptote as $p_{T,\text{jet}}^v \rightarrow \infty$ around which we perform a series expansion:

$$\rho(p_{T,\text{jet}}^v, \Delta^{\text{ref}}, \Delta^v) = \sqrt{F_{\text{pert}}} \frac{p_{T,\text{jet}}^{\text{ref}}}{p_{T,\text{jet}}^{\text{ref}} + \Delta^{\text{ref}}} \left(1 - \frac{2p_{T,\text{jet}}^{\text{ref}} \Delta^{\text{ref}} + (\Delta^{\text{ref}})^2}{2(p_{T,\text{jet}}^v)^2} + \frac{(p_{T,\text{jet}}^{\text{ref}} + \Delta^{\text{ref}})^2 (\Delta^{\text{ref}} + \Delta^v)}{8(p_{T,\text{jet}}^v)^3} + \mathcal{O}\left(\frac{1}{(p_{T,\text{jet}}^v)^4}\right) \right). \quad (27)$$

Thus a fit of the asymptote of ρ , and its first non-zero correction, can be used to extract F_{pert} and Δ^{ref} . All dependence on Δ^v enters in the higher order terms. However, in the limit that $p_{T,\text{jet}}^{\text{ref}} \rightarrow \infty$, $\rho^2 \rightarrow F_{\text{pert}}$ and so while the fit for F_{pert} will become exact, the error on a fit for Δ^{ref} will diverge. In practice it will be necessary to perform the EEEEC measurement with boosted tops in order to get a well-defined peak. Consequently, fits for Δ^{ref} will suffer from parametrically large errors (as can be seen in the large deviation between the exact and expanded curves at low $p_{T,\text{jet}}^{\text{ref}}$

PYTHIA8 m_t	EEEC Parton $\sqrt{F_{\text{pert}}}$	EEEC Hadron $\sqrt{F_{\text{pert}}}$	EEEC Hadron + MPI $\sqrt{F_{\text{pert}}}$
172 GeV	172.6 ± 0.3 GeV	$172.4 \pm 0.2 \pm 0.5$ GeV	$172.3 \pm 0.2 \pm 0.4$ GeV
173 GeV	173.5 ± 0.3 GeV	$173.9 \pm 0.3 \pm 0.5$ GeV	$173.6 \pm 0.2 \pm 0.4$ GeV
173 – 172	0.9 ± 0.4 GeV	1.5 ± 0.8 GeV	1.3 ± 0.6 GeV

TABLE II: A more detailed version of the Table shown in the main text, showing separate results at parton, hadron and hadron+MPI level. Five data sets for ρ were averaged over with $p_{T,\text{jet}}^{\text{ref}} \in [550, 650]$ GeV binned in 20 GeV intervals and $p_{T,\text{jet}}^v \in [900, 2000]$ GeV. One such data set and its fit is shown in Fig. 7. In each column the first error is from the fit of the ρ asymptote and is statistical. The second error (when given) is also statistical and is the error from using the parton shower to determine $\Delta'^{\text{ref}} \approx \Delta^{\text{ref}}$ as extracted from the top jet p_t distribution. Errors have been combined in quadrature in the final row. No theory errors are given.

in Fig. 7). However, as previously stated, Δ^{ref} can be extracted from an independent measurement of the top-jet p_T distribution,

$$\frac{d\sigma_{pp \rightarrow t(\rightarrow b\bar{q}\bar{q}') + X}}{dp_{T,\text{jet}}^{\text{ref}}} = D(m_t, p_{T,\text{jet}}, \alpha_s, \Lambda_{\text{QCD}}). \quad (28)$$

One can parameterize the non-perturbative effects in D in the same way as we did in $\zeta_{\text{peak}}^{(pp)}$ to give

$$D(m_t, p_{T,\text{jet}}, \alpha_s, \Lambda_{\text{QCD}}) = D^{\text{pert.}}(m_t, g(p_{T,\text{jet}}, m_t, \alpha_s, \Lambda_{\text{QCD}}), \alpha_s),$$

where $D^{\text{pert.}}(m_t, p_{T,\text{jet}}, \alpha_s)$ is the all-orders perturbative top-jet p_T distribution, and $g(p_{T,\text{jet}}, \dots)$ captures all the non-perturbative modifications to $p_{T,\text{jet}}$. As before, we parameterize the modifications via introducing a shift function Δ' defined as

$$\Delta'(p_{T,\text{jet}}, m_t, \alpha_s, \Lambda_{\text{QCD}}) \equiv g(p_{T,\text{jet}}, m_t, \alpha_s, \Lambda_{\text{QCD}}) - p_{T,\text{jet}}, \quad \text{and} \quad \Delta'^{\text{ref}} \equiv g(p_{T,\text{jet}}^{\text{ref}}, m_t, \alpha_s, \Lambda_{\text{QCD}}) - p_{T,\text{jet}}^{\text{ref}}. \quad (29)$$

It is required for consistency with the factorization in Eq. (10) that, up to corrections which are suppressed by powers of $m_t/p_{T,\text{jet}}^{\text{ref}}$ and $\Lambda_{\text{QCD}}/p_{T,\text{jet}}^{\text{ref}}$, $\Delta'^{\text{ref}} \approx (\Delta^{\text{ref}} - \Delta_{\text{pert}}^{\text{ref}})$ where $\Delta_{\text{pert}}^{\text{ref}}$ is the perturbative contribution to Δ^{ref} . At the level of accuracy to which we are working, $\Delta_{\text{pert}}^{\text{ref}}$ can be absorbed into F_{pert} and so we drop it from the rest of this section and in the main body of this *Letter*.

Thus, we fit for F_{pert} using the following procedure:

1. We fit for the asymptote of ρ (which we label ρ_{asy}) using a polynomial in $(1/p_{T,\text{jet}}^v)^n$. In this paper we found that a third degree polynomial, $\rho = \rho_{\text{asy}} + c_2(p_{T,\text{jet}}^v)^{-2} + c_3(p_{T,\text{jet}}^v)^{-3}$, optimized the reduced χ^2 . The value of ρ_{asy} was found to be stable, within our statistical accuracy, against the inclusion of further higher order terms, $c_n(p_{T,\text{jet}}^v)^{-n}$. Fig. 7 shows one such fit.
2. We extract Δ'^{ref} from the top-jet p_T spectrum. Fig. 8 shows the extraction of Δ'^{ref} from the jet $p_{T,\text{jet}}$ spectrum.
3. Finally, we compute F_{pert} as

$$\sqrt{F_{\text{pert}}} = \rho_{\text{asy}} \frac{p_{T,\text{jet}}^{\text{ref}} + \Delta'^{\text{ref}}}{p_{T,\text{jet}}^{\text{ref}}}. \quad (30)$$

The outcome of this procedure is given in Table II which shows the extracted F_{pert} from PYTHIA8 with $m_t = 172$ GeV and 173 GeV. The important outcome of this analysis is that the differences between the measured masses with parton, hadron and hadron+MPI data are $\lesssim 1$ GeV and are smaller than the statistical errors. This analysis was not optimized to give a good statistical error and certainly can be improved. Thus we find promising evidence that complete theoretical control of the top mass, up to errors < 1 GeV, is possible with an EEEC based measurement.

To cross-check our result, in Fig. 9 we illustrate a theory fit of ρ using parton shower data from PYTHIA8 with $m_t = 172$ GeV at parton level, hadron level and hadron level + MPI. The fit in Fig. 9 is *not* the third degree polynomial used to extract ρ_{asy} . Rather, the fit uses the values of F_{pert} given in Table II and the values of Δ'^{ref} given in Fig. 8 as an input into the expansion given in Eq. (27), truncated at second order. Error bars correspond to the errors on F_{pert} and Δ'^{ref} . We find agreement between the MC data and our theory fit. Fig. 10 further demonstrates the excellent agreement between theory and parton shower data wherein we fit $\zeta_{\text{peak}}(p_{t,\text{jet}})$ with the ansatz in Eq. (9) also using the values for F_{pert} in Table II and the values of Δ'^{ref} given in Fig. 8.

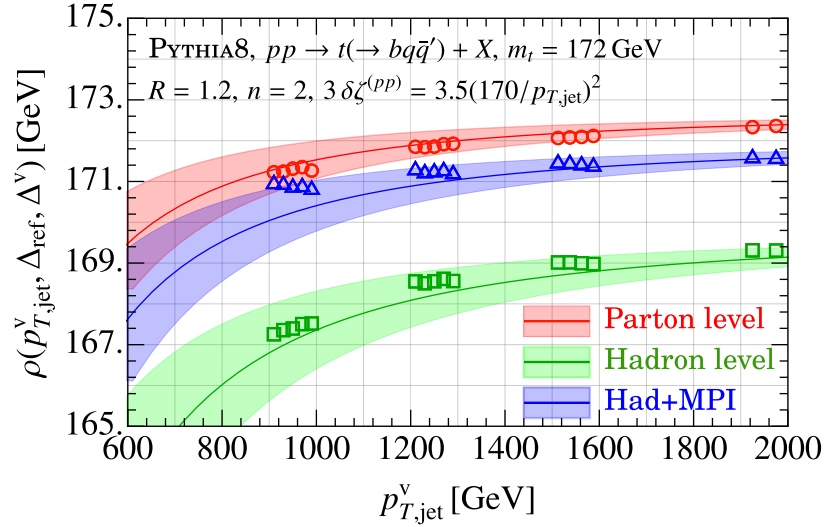


FIG. 9: This figure shows parton shower data for ρ generated in PYTHIA8 at parton level, hadron level, and with MPI (shown in open markers) overlaid with a theory fit. Five data sets for ρ were averaged over with $p_{T,jet}^{\text{ref}} \in [550, 650]$ GeV binned in 20 GeV intervals. The theory fit is of the second order expansion of ρ (which we label $\rho^{(2)}$) with, as input, the values of F_{pert} given in Table II and the values of Δ^{ref} given in Fig. 8. The theory fit is a cross-check of our analysis, it was not used to determine F_{pert} . To illustrate the partonic theory fit, a value of $\Delta_{\text{pert}}^{\text{ref}} = (11 \pm 3)\text{GeV}$ has been extracted, as expected with a large error, from the fit for $\rho^{(2)}$. This $\Delta_{\text{pert}}^{\text{ref}}$ is not used in the rest of the analysis where all dependence on $\Delta_{\text{pert}}^{\text{ref}}$ is absorbed in to the definition of F_{pert} . Each error band shows the combined statistical error from the determination of the asymptote and of Δ^{ref} (including the dominant error on $\Delta_{\text{pert}}^{\text{ref}}$).

Zoomed-In Distributions for e^+e^-

In the figures presented in the main text, we focused primarily on the global structure of the peaks in the EEEC distribution. To get a better feeling for the shift due to hadronization, it is also useful to have a zoomed in plot of the peak region. This is shown in Fig. 11 for the $n = 2$ three-point correlator in e^+e^- for two top mass values, and at both hadron and parton level. From the peak positions in these curves we deduce that the hadronization effects shift the top mass by $\Delta m_t^{\text{Had.}} \sim 250$ MeV.

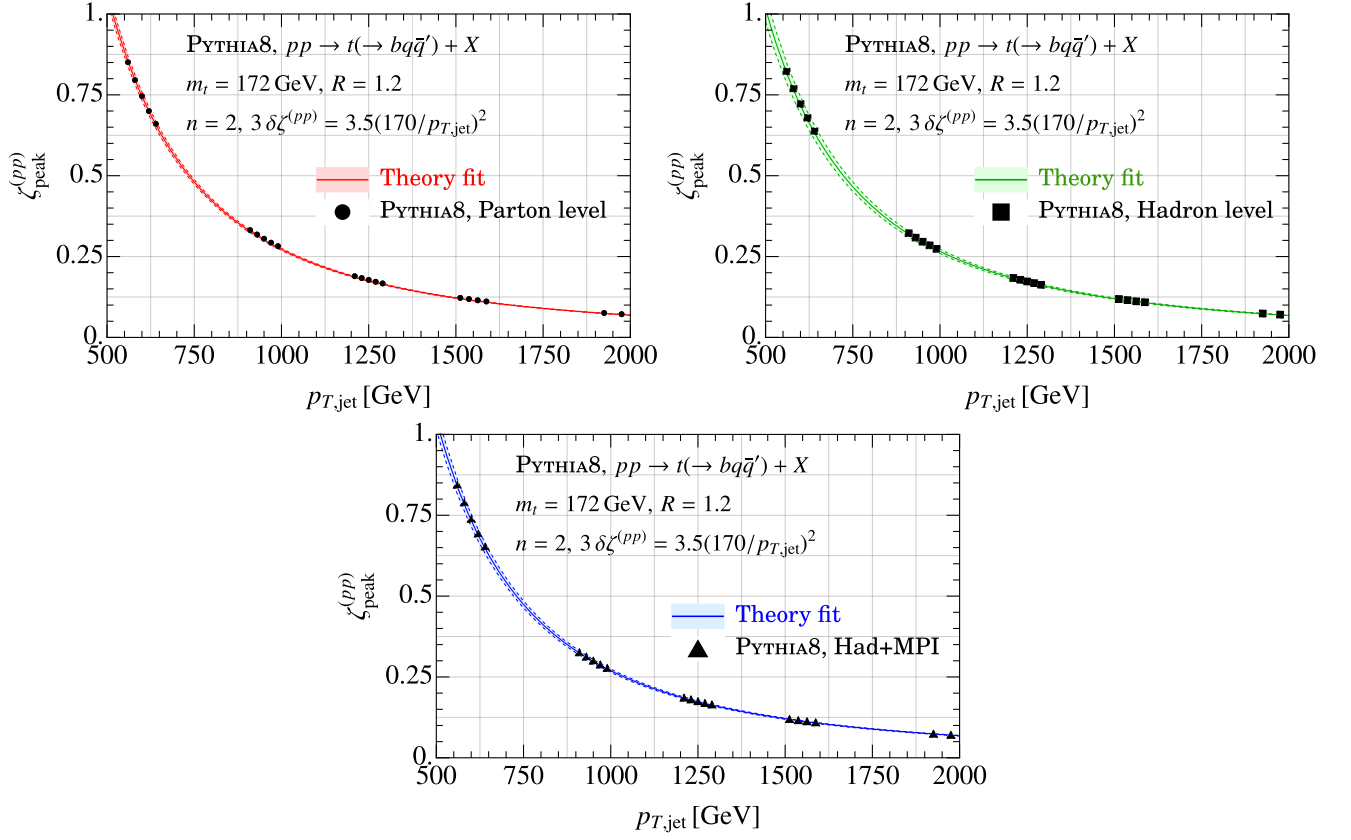


FIG. 10: Energy correlator peak positions as a function of $p_{T,\text{jet}}$ at parton level, hadron level, and including MPI. The theory fit uses the ansatz in Eq. (9) with the values of F_{pert} given in Table II and Δ^{ref} extracted in Fig. 8. Excellent agreement between the theoretical fit and PYTHIA8 is observed in all cases.

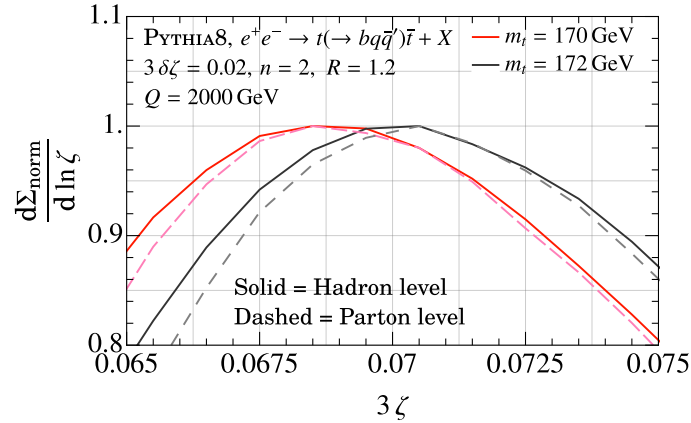


FIG. 11: A zoomed-in plot of the $n = 2$ three-point correlator in e^+e^- for $m_t = 170, 172$ GeV, at both hadron and parton level.